Vol 17 No 6, June 2008
1674-1056/2008/17(06)/2240-05

Chinese Physics B

© 2008 Chin. Phys. Soc.
and IOP Publishing Ltd

Preparation of p-type ZnO:(Al, N) by a combination of sol–gel and ion-implantation techniques*

Xue Shu-Wen(薛书文)[a)b)†], Zu Xiao-Tao(祖小涛)[a)], Shao Le-Xi(邵乐喜)[b)], Yuan Zhao-Lin(袁兆林)[a)], Xiang Xia(向 霞)[a)], and Deng Hong(邓 宏)[c)]

[a)] *Department of Applied Physics, University of Electronic Science and Technology of China, Chengdu* 610054, *China*
[b)] *Department of Physics, Zhanjiang Normal College, Zhanjiang* 524048, *China*
[c)] *School of Microelectronics and Solid-state Electronics, University of Electronic Science and Technology of China, Chengdu* 610054, *China*

(Received 22 October 2007; revised manuscript received 10 December 2007)

We report the preparation of p-type ZnO thin films on (0001) sapphire substrates by a combination of sol–gel and ion-implantation techniques. The results of the Hall-effect measurements carried out at room temperature indicate that the N-implanted ZnO:Al films annealed at 600°C have converted to p-type conduction with a hole concentration of $1.6\times10^{18}\,\mathrm{cm}^{-3}$, a hole mobility of $3.67\,\mathrm{cm}^2/\mathrm{V}\cdot\mathrm{s}$ and a minimum resistivity of $4.80\,\mathrm{cm}\cdot\Omega$. Ion-beam induced damage recovery has been investigated by x-ray diffraction (XRD), photoluminescence (PL) and optical transmittance measurements. Results show that diffraction peaks and PL intensities are decreased by N ion implantation, but they nearly recover after annealing at 600°C. Our results demonstrate a promising approach to fabricate p-type ZnO at a low cost.

Keywords: ZnO, ion implantation, XRD
PACC: 7155F, 7855D, 0765E

1. Introduction

ZnO has recently attracted much attention because it has some interesting physical properties suitable for short-wavelength optoelectronic device applications, such as blue and ultraviolet (UV) lasers, light-emitting diodes, and solar cells.[1−3] Though ZnO already has many industrial applications owing to its piezoelectric properties and its band gap being in the near ultraviolet, the main obstacle to the development of ZnO has been the lack of reproducible and low-resistivity p-type ZnO. In recent years, many techniques have been widely employed to synthesize ZnO films, such as radio frequency (RF) magnetron sputtering, chemical vapor deposition, pulsed laser deposition, plasma-assisted molecular beam epitaxy (MBE), and the sol–gel process.[4−8] Among these techniques, the sol–gel chemical deposition technique is very attractive as it can be implemented easily in a laboratory for the deposition of semiconducting thin films. This technique offers the possibility of preparing a small- as well as large-area coating of ZnO thin films at a low cost for technological applications.

Recent theoretical and experimental studies show that nitrogen is a very promising p-type dopant, but its solubility in ZnO is low. Ion implantation and donor-acceptor co-doping method are two effective approaches to enhance the solubility limit of nitrogen in ZnO. Ion implantation is a widespread tool for doping semiconductors in the semiconductor industry. Advantages of ion implantation are the lateral selectivity of sample area and doping depth as well as an accurate fluence control. Despite the wide applications of ion implantation in semiconducting industry, only several groups have claimed p-type conduction in ZnO by As and N ion implantation.[9−11]

In this paper, we report N ion implantation into ZnO:Al films by the sol–gel process. The influences of N ion implantation and post-thermal annealing on ZnO:Al films are investigated.

2. Experimental

2.1. Preparation of ZnO:Al films and N-ion-implantation

ZnO:Al thin films used in this study were deposited on (0001) sapphire substrates by

*Project supported by the Program for New Century Excellent Talents in University (Grant No NCET-04-0899) and Special Foundation for University Subject Construction, Department of Education of Guangdong Province, China (Grant No [2006] 11).
†E-mail:xueshuwen@263.net

the sol–gel method. Zinc acetate dehydrate ($Zn(CH_3COO)_2{\cdot}H_2O$) was used as a starting material. Monoethanolamine (MEA) and 2-methoxyethanol were used as stabilizer and solvent, respectively. The Al dopant source is $Al(NO_3)_3{\cdot}9H_2O$. For Al doping, zinc acetate dehydrate and $Al(NO_3)_3{\cdot}9H_2O$ were first dissolved in a mixture of 2-methoxyethanol and MEA solution at room temperature. The atomic ratio of Al/Zn was kept at 0.01:1.00, and the molar ratio of MEA to zinc acetate ($Zn(CH_3COO)_2$) was maintained at 1.0, with the concentration of zinc acetate being 0.35 mol/L. The solution was stirred at 60°C for 2 h to yield a clear and homogeneous solution, which served as the coating solution after cooling to room temperature. Usually the coating was made 24 hours after the solution was prepared. Then the solution was dropped onto (0001) sapphire substrates, which were made rotating at 4000 rpm for 30 s. After depositing by spin coating, the films were dried at 300°C for 10 min on a hot plate to evaporate the solvent and remove organic residuals. The procedures from coating to drying were repeated twelve times. After that the films were put into a quartz tube furnace and annealed in air at 500°C for 1 h. The average thickness of the films chosen was about 800 nm, measured by an OLYMPUS BX51 interference/transmission microscope.

The as-prepared ZnO:Al films were subjected to N ion implantation with a fluence of $1 \times 10^{17} N^+/cm^2$. The acceleration voltage and dose rate for N^+ ions were 56 kV and $\sim 2\mu A/cm^2$, respectively. Figure 1 shows the depth profile of implanted N atoms obtained by simulation using the code TRIM 96. The projected range (R_p) of the atoms is about 104.9 nm. After ion implantation, N-implanted films were annealed in flowing nitrogen at 500–900°C for 30 min in a quartz tube furnace.

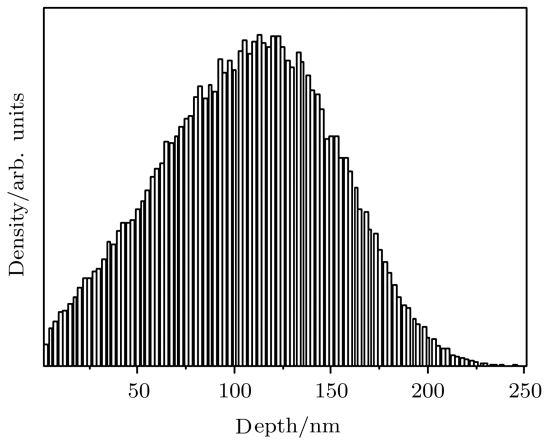


Fig.1. TRIM simulation of the depth profile of implanted N atoms for ZnO:Al films.

2.2. Measurements

To characterize the structural and optical properties of the as-prepared and N-implanted films, the crystal orientation was investigated using a PHILIPS X'PERT PRO MPD x-ray diffractometer (XRD) with the radiation source of CuKα. Optical absorbance was measured using a SHIMADZU UV2550 spectrophotometer. Room temperature (RT) photoluminescence spectra (PL) were recorded by a SHIMADZU RF5301PC spectrophotometer with excitation wavelength of 345 nm. The resistivity of the films was measured by the four-point probe method. RT Hall-effect measurement was made with HEM-2000 (magnetic field strength: 0.37 T). Before electrical measurements, silver spot electrodes were made on ZnO films and the ohmic contact between electrodes and films was confirmed.

3. Results and discussion

3.1. Structural properties

To investigate the effects of annealing on the structural properties of N-implanted ZnO:Al films, the films were annealed in flowing nitrogen at different temperatures from 500 to 900°C for 30 min after N ion implantation. Figure 2 shows XRD patterns of ZnO:Al films after N ion implantation and subsequent thermal annealing at different temperatures. For comparison, we also add XRD patterns of ZnO:Al films before and after N ion implantation. It can be seen that all films still show the hexagonal wurtzite structure after N ion implantation and post-thermal annealing. No evidences of any other secondary phases and impurities are found in the XRD patterns. Though ZnO is a radiation-hard material, we can see that the intensities of all diffraction peaks are greatly decreased by N ion implantation. The decreases of diffraction peaks can be attributed to ion-beam induced lattice disorder. Thermal annealing has evident influences on the structural properties of N-implanted films. Figure 2 shows that the diffraction peaks of N-implanted ZnO:Al films increase with increasing annealing temperature from 500–800°C. Similar results are also found in Zn-implanted ZnO films.[12] We attribute the

enhancement of diffraction peaks to the annealing-out of ion-beam induced defects and re-crystallization after annealing. However, the intensities of all peaks decrease when annealing temperature exceeds 800°C. The decreases of all peaks can be attributed mainly to the thermal induced lattice disorder at high temperatures. It is noted that the diffraction peaks nearly recover after annealing at 600°C. This suggests that most of ion-beam induced defects have been annealed out at this stage.

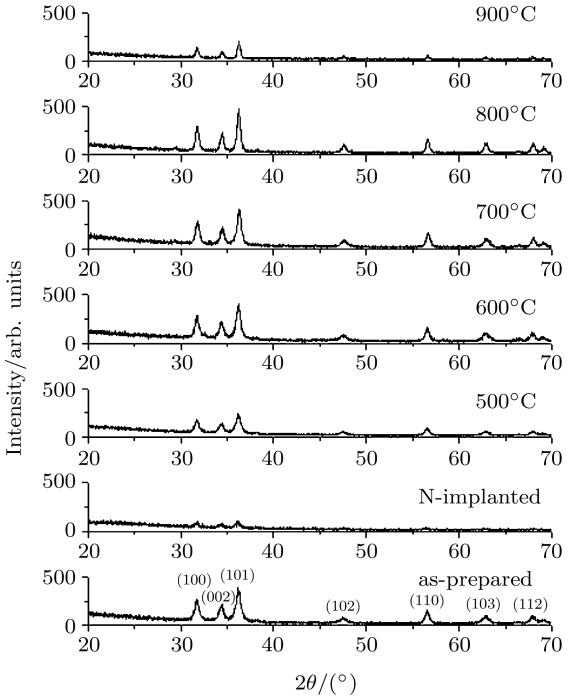


Fig.2. XRD patterns of ZnO:Al films after N-implantation and post-thermal, annealed at different temperatures.

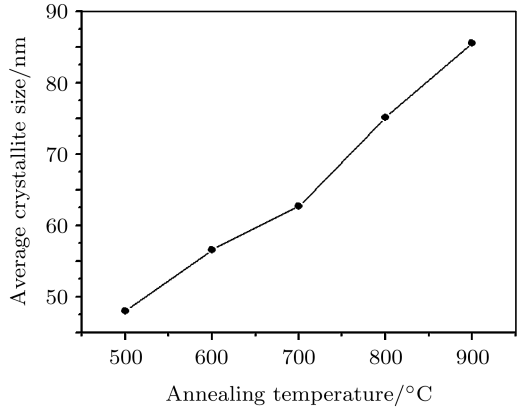


Fig.3. Average crystallite size for different annealing temperatures.

In addition, post-thermal annealing also has pronounced effects on the crystallite size of N-implanted ZnO:Al films. We have calculated the average crystallite sizes of N-implanted ZnO:Al films from the full width at half maximum (FWHM) of (002) peak at various annealing stages. The calculated results are plotted in Fig.3. It can be seen that the average crystallite size increases with increasing annealing temperature.

3.2. Optical properties

Figure 4 shows the influences of N ion implantation and post-thermal annealing on the optical transmittance of N-implanted ZnO:Al films. It can be seen from Fig.4 that the optical transmittance decreases distinctly in the visible region after N ion implantation. Subsequent annealing has evident influences on the optical transmittance of N-implanted ZnO:Al films. It is found that the optical transmittance in the visible region increases with increasing annealing temperature from 500–800°C, while decrease slightly when annealing temperature exceeds 800°C. We have also observed similar results in Zn-implanted ZnO films and N-implanted ZnO:Mg films. As mentioned in the structural analysis, many defects are produced during ion implantation and high-temperature annealing. These defects may serve as trapped electron centres and can effectively affect optical absorption.[13,14] Therefore, we ascribe the increase and decrease of optical transmittance mainly to the annealing out of ion-beam induced defects and the production of thermal induced defects at high temperatures, respectively.

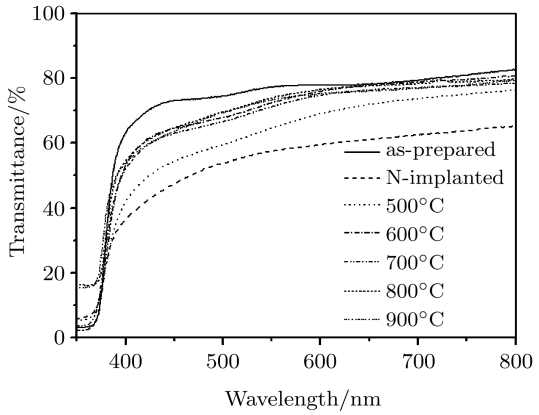


Fig.4. Transmittance spectra of N-implanted ZnO:Al annealed at different temperatures.

N ion implantation and post-thermal annealing also have evident influences on the optical bandgaps of ZnO:Al films as shown in Figs.5 and 6. The optical bandgaps are determined from the conventional method.[15] It can be seen that the optical bandgap

redshifts after N ion implantation. Subsequent annealing at a temperature between 500 and 700°C makes the optical bandgap blueshift, but redshift when annealing temperature exceeds 700°C. Similar results are also found in Zn-implanted ZnO films [12] and N-implanted ZnO:Mg films. We also attribute the observed behaviours of the optical bandgaps mainly to the changes of defect concentrations in ZnO films. As discussed above, many defects are produced during N ion implantation. They may cause the redshift of the optical bandgap. Most of the ion-beam induced defects are annealed out by the subsequent annealing at temperatures from 500 to 700°C. This results in the blueshift of bandgap due to the decrease of defect concentration in ZnO:Al films. During the following annealing stage between 700 and 900°C, thermal induced defects at high temperatures increase dramatically, leading to the redshift of the optical band edge again due to the increase of defect concentration.

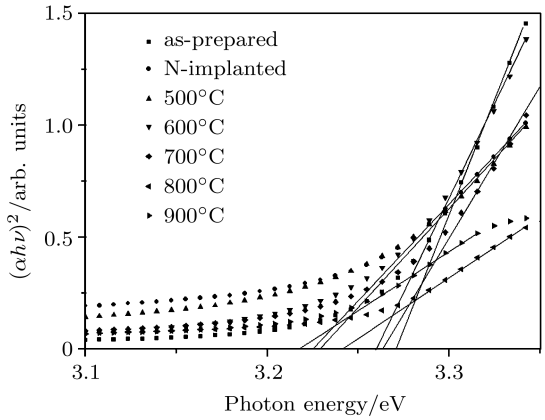


Fig.5. $(\alpha h\nu)^2 - h\nu$ plots of N-implanted ZnO:Al films annealed at different temperatures.

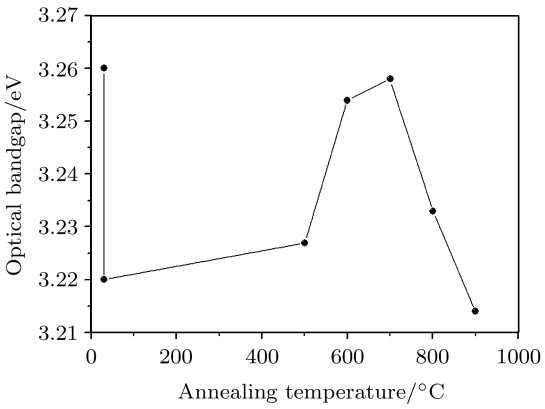


Fig.6. Bandgaps of N-implanted ZnO:Al films annealed at different temperatures.

In Fig.7 are shown RT PL spectra of ZnO:Al films after ion implantation and annealing at different temperatures from 500 to 900°C. The shape of all the spectra, similar to those reported by others in Refs.[16–18], is featured by a near band edge (NBE) excitonic UV emission and a defect-related deep level emission (DLE) in the visible region. It can be seen that NBE and DLE are decreased after N ion implantation, and the decreases are mainly due to the ion-beam induced defects which serve as non-radiative centres.[19] Compared with Ref.[19] it is noted that PL emission is not completely extinguished in our experiment. We have observed similar results in Zn-implanted ZnO films and N-implanted ZnO:Mg films. We think that this difference may be due to different implantation conditions and properties of the material used in the experiments (single crystal ZnO was used in Ref.[19]). Subsequent annealing has pronounced influences on the emission properties. Both NBE and DLE are enhanced with increasing annealing temperatures from 500 to 900°C. It can be found in Fig.7 that the NBE and DLE nearly recover after annealing at 600°C.

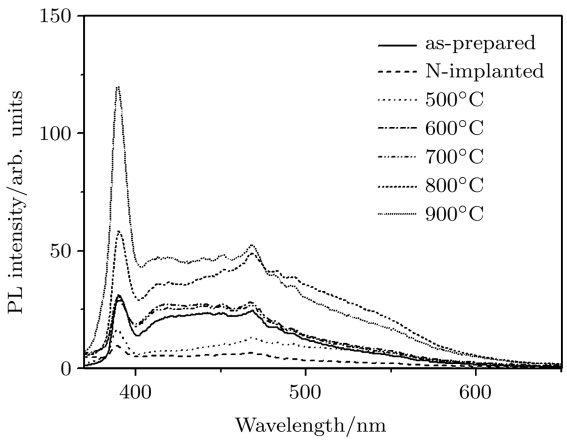


Fig.7. RT Photoluminescence spectra of N-implanted ZnO:Al annealed at different temperatures (Excitation wavelength: 345 nm).

3.3. Electrical properties

We have monitored the resistivity of N-implanted ZnO:Al films with four-point probe method at every stage. The results are listed in Table 1. It can be seen that the resistivity of N-implanted ZnO:Al films decreases with increasing annealing temperatures from 500–600°C, but increases when annealing temperature exceeds 600°C. The resistivity reaches its minimum

after annealing at 600°C. At this stage, we make RT Hall-effect measurement of N-implanted ZnO:Al films. The results confirm that the films are of p-type conduction, in which the hole concentration and mobility are $1.6 \times 10^{18}\,\mathrm{cm}^{-3}$ and $3.76\,\mathrm{cm}^2/\mathrm{V}\cdot\mathrm{s}$, respectively. The observed increase of the resistivity of N-implanted ZnO:Al films with increasing annealing temperature is believed to be due to the rapid production of oxygen vacancy at high temperatures, which compensates, the acceptors in the films, while the decrease may be due to the activation of the acceptors. However, this is purely speculative, and further work is necessary.

Table 1. The resistivity of N-implanted ZnO:Al films with annealing temperatures.

Annealing temperature /°C	500	600	700	800	900
Resistivity / Ω· cm	2.35×10^2	4.80	1.62×10^2	2.37×10^3	8.73×10^4

4. Conclusions

N-ion-implantation with a fluence of $1\times 10^{17}\mathrm{N}^+/\mathrm{cm}^2$ are performed on ZnO:Al thin films deposited on (0001) sapphire substrates by the sol–gel technique. After N-implantation of ZnO:Al films, the films are annealed in flowing nitrogen at 500–900°C. Damage recovery are investigated by x-ray diffraction (XRD), photoluminescence (PL) and optical absorption measurements. Results show that diffraction peaks and PL intensities are decreased by N ion implantation, but they nearly recover by further annealing at 600°C. The Hall-effect measurements confirm that the N-implanted ZnO:Al films annealed at 600°C exhibits p-type conduction with a hole concentration of $1.6 \times 10^{18}\,\mathrm{cm}^{-3}$, a hole mobility of $3.67\,\mathrm{cm}^2/\mathrm{V}\cdot\mathrm{s}$ and a minimum resistivity of $4.80\,\mathrm{cm}\cdot\Omega$.

References

[1] Look D C 2001 *Mater. Sci. Eng.* B **80** 383

[2] Huang M H, Mao S, Feick H, Yan H Q, Wu Y Y, Kind H, Weber E, Russo R and Yang P 2001 *Science* **292** 1897

[3] Pearton S J, Norton N P, Ip K, Heo Y W and Steiner T 2005 *Prog. Mater. Sci.* **50** 293

[4] Zhou X, Wang S Q, Lian G J and Xiong G C 2006 *Chin. Phys.* **15** 199

[5] Yao Z G, Zhang X Q, Shang H K, Teng X Y, Wang Y S and Huang S H 2005 *Chin. Phys.* **14** 1205

[6] Wang Z J, Wang Z J, Li S C, Wang Z H, Lu Y M and Yuan J S 2004 *Chin. Phys.* **13** 750

[7] Monteiro T, Boemare C, Soares M J, Rita E and Elves E 2003 *J. Appl. Phys.* **93** 8995

[8] Xue S W, Zu X T, Su H Q, Xiang X, Deng H and Yang C Y 2007 *Chin. Phys.* **16** 1119

[9] Lin C C, Chen S Y, Cheng S Y and Lee H Y 2004 *Appl. Phys. Lett.* **84** 5040

[10] Georgobiani A N, Gruzintsev A N, Volkov V T, Vorobiev M O, Demin V I and Dravin V A 2003 *Nucl. Instrum. Methods Phys. Res.* A **514** 117

[11] Jeong T S, Han M S, Youn C J and Park Y S 2004 *J. Appl. Phys.* **96** 175

[12] Xue S W, Zu X T, Shao L X, Yuan Z L, Zheng W G, Jiang X D and Deng H 2007 *J. Alloys and Compounds*

[13] Mackey J H, Smith H L and Halperin A 1966 *J. Phys. Chem. Solids* **27** 1759

[14] Cohen A J and Janezic G G 1983 *Phys. Stat. Sol.* A **77** 619

[15] Kenny N, Kannewurf C R and Whitmore D H 1966 *J. Phys. Chem. Solids* **27** 1237

[16] Fujihara S, Ogawa Y and Kasai A 2004 *Chem. Mater.* **16** 2965

[17] Gao X D, Li X M and Yu W D 2005 *Mater. Res. Bull.* **40** 1104

[18] Hong R J, Shao J D, He H B and Fan Z X 2006 *J. Crystal Growth* **290** 334

[19] Sakaguchi I, Park D, Takata Y, Hishita S, Ohashi N, Haneda H and Mitsuhashi T 2003 *Nucl. Instrum. Methods Phys. Res.* B **206** 153